Strong biquadratic coupling and antiferromagnetic-ferromagnetic crossover in NiFe/Cu multilayers

K. Pettit
Department of Physics, University of Illinois at Urbana Champaign, 1110 W. Green Street, Urbana, Illinois 61801-3080 and IBM Research Division, Almaden Research Center, 650 Harry Road, San Jose, California 95120-6099

S. Gider and S. S. P. Parkin
IBM Research Division, Almaden Research Center, 650 Harry Road, San Jose, California 95120-6099

M. B. Salamon
Department of Physics, University of Illinois at Urbana Champaign, 1110 West Green Street, Urbana, Illinois 61801-3080 and Center for Materials Science, Los Alamos National Laboratory, Los Alamos, New Mexico 87545
(Received 4 November 1996; revised manuscript received 22 May 1997)

We report clear manifestations of biquadratic exchange in the magnetoresistance (MR) of (110) single-crystal NiFe/Cu multilayers. Magnetoresistance curves show a low-field MR minimum which results from an asymmetric canting of the moments away from the applied magnetic field. The stability of these magnetic configurations indicates that the biquadratic coupling can be significantly stronger than the bilinear coupling. In samples with ferromagnetic (F) bilinear coupling the strength of both the bilinear and biquadratic coupling decays in the temperature range from 200 to 400 K. In samples that are coupled antiferromagnetically (AF) at room temperature, we observe a crossover from AF to F bilinear coupling as the temperature is lowered below 200 K. We attribute the strong biquadratic coupling and temperature dependence of the bilinear coupling to pinholes in the Cu spacer layers. [S0163-1829(97)07437-7]

In recent years, the coupling between ultrathin (≈ 10 Å) transition-metal ferromagnetic films, separated by nonmagnetic spacer layers, has been studied intensely.[1] It was generally assumed and observed that the interaction between the magnetic moments $\mathbf{m}_1 = m\hat{\mathbf{n}}_1$ and $\mathbf{m}_2 = m\hat{\mathbf{n}}_2$ was proportional to $\hat{\mathbf{n}}_1 \cdot \hat{\mathbf{n}}_2$. This is termed *bilinear* exchange and positive bilinear exchange favors antiparallel alignment of the $\mathbf{m}_i$. Interest in this subject has been spurred by the large changes in resistance that can occur when the antiparallel $\mathbf{m}_i$ align in a magnetic field, the giant magnetoresistance (GMR) effect.[2] More recently, a second-order *biquadratic* interaction, which favors orthogonal alignment of successive $\mathbf{m}_i$, has been studied and observed.[3–7] The effects of biquadratic coupling on the magnetic phase diagram and the magnetoresistance have been treated theoretically, primarily in the presence of antiferromagnetic bilinear exchange and magnetic anisotropy.[8–10]

In this paper, we report a reentrant magnetoresistive effect that signifies the presence of dominant biquadratic coupling and permits us to determine the biquadratic and bilinear coupling strengths. We use the well-documented oscillation of the bilinear coupling with spacer layer thickness and tune that coupling to be weakly ferromagnetic.[1,2] In the presence of such weak, negative bilinear coupling, the magnetoresistance shows a sharp minimum with respect to fields applied along the hard direction. Such behavior cannot result from bilinear exchange alone; rather, it is a result of biquadratic coupling in cooperation with magnetic anisotropy.[9] The biquadratic coupling strength in these samples is significantly stronger than both intrinsic[6,11,12] and extrinsic[7,13,14] models of biquadratic coupling predict. We also observe a crossover from antiferromagnetic to ferromagnetic bilinear coupling, previously unseen in transition-metal multilayers with nonmagnetic spacer layers.[15] This observation gives some clues as to the origin of the strong biquadratic coupling.

The multilayered samples used in this study are composed of 20 20-Å layers of Permalloy ($Ni_{79}Fe_{21}$) separated by Cu spacers of varying thickness. The samples were grown by dc magnetron sputtering from Permalloy and Cu targets. In order to induce in-plane uniaxial magnetic anisotropy, the samples were prepared on MgO (110) substrates, on which Fe and Pt seed layers were first grown at a substrate temperature of ≈ 450 °C to ensure high quality fcc growth. The subsequent layers were deposited at ≈ 40 °C. The sample structures are MgO(110)/Fe(5 Å)/Pt(45 Å)/Cu(t_{Cu})/ [$Ni_{71}Fe_{21}$(20 Å)/Cu(t_{Cu})$]_{20}$/Pt(45 Å), where t_{Cu} is the thickness of the Cu spacer layer. The multilayers are single crystals and have the [110] (hard direction) and [100] (easy direction) axes in the sample plane. Resistivity data were obtained using a conventional four-contact ac lock-in method with the field along both easy and hard directions. Magnetization data were obtained using a superconducting quantum interference device-based magnetometer and a magneto-optic Kerr effect polarimeter.

Figure 1 is a plot of the room-temperature magnetoresistance, $\Delta R(H)/R_s$, of four samples with t_{Cu}=9, 10, 11, and 13 Å; R_s is the resistance at magnetic saturation. The inset shows the Kerr rotation at low fields for three of the samples. The field is applied along the hard [110] axis and the current along the easy [100] axis. Measurements at other angles confirmed that there is a single hard axis in the film plane. The saturation field and hence coupling strength is largest for t_{Cu} =11 Å; however, the maximum MR occurs at t_{Cu}=13 Å where the parabolic MR curve and zero remanent magnetization are characteristic of complete antiparallel alignment of adjacent magnetic moments at zero field.[8] We will show that the cusped MR curve of the t_{Cu} =11 Å sample, and espe-

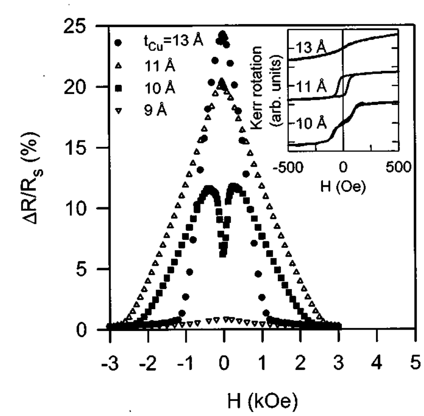

FIG. 1. The magnetoresistance vs applied magnetic field for four NiFe/Cu multilayers of different Cu spacer-layer thickness. The inset shows the Kerr magnetization loops for three of the samples. The field is applied along the hard axis.

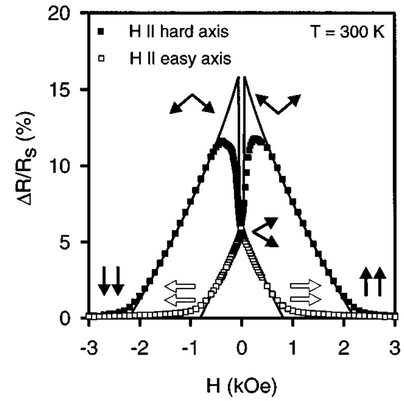

FIG. 2. The magnetoresistance vs applied magnetic-field plots for the NiFe/Cu multilayer with t_{Cu}=10 Å. The magnetic field was applied along both the easy and hard directions of magnetization. The solid lines are results of a numerical simulation described in the text. The arrows indicate the direction of magnetization in alternate layers. Dark arrows are for the field along the hard axis, light arrows are for the field along the easy axis.

cially the reentrant MR shape of the $t_{Cu}=10$ Å are indicative of biquadratic coupling. We have observed the latter effect in these and other multilayers only in a narrow range of spacer-layer thicknesses close to the points at which the bilinear exchange changes sign. The t_{Cu}=9 Å sample is ferromagnetic and its MR is characteristic of the individual permalloy layers.

The complex magnetoresistive behavior of the t_{Cu}=10 Å sample occurs only for fields applied along the hard axis, as demonstrated in Fig. 2. There is little hysteresis ($\leqslant$30 Oe) when the field is applied in either direction. Note the hard-axis MR maximum is nearly double the easy-axis MR maximum.

In the simplest picture of the GMR effect, the MR depends only on the angle $\xi=\cos^{-1}(\hat{\mathbf{n}}_i\cdot\hat{\mathbf{n}}_{i+1})$ between successive ferromagnetic moments.[1,2] Since this angle may take on an arbitrary value ξ_o at zero field, we write the MR as

$$\frac{\Delta R(\xi)}{R_s}=\left(\frac{R_o}{R_s}-1\right)\left(\frac{\sin^2(\xi/2)}{\sin^2(\xi_o/2)}\right), \tag{1}$$

where $R_o=R(\xi_o)$. The data for the t_{Cu}=10 Å sample in Fig. 2 suggest that ξ is smaller at zero field than it is at higher fields (around 500 Oe) when the field is applied along the hard direction.

To better understand the origin of this MR minimum, we consider the total energy of the system, the minimum of which determines the equilibrium configuration of the magnetic moments. Although in a real system domain nucleation, growth, and domain-wall motion complicate the magnetization process, we will assume that the moment of each ferromagnetic layer is rigid and confined to the sample plane, that the magnetization process occurs by rotation of these layers, and that the system always evolves to the global energy minimum. In a system of two identical ferromagnetic layers of thickness t in a magnetic field **H** the ''reduced'' total energy per unit volume $\varepsilon\equiv 2E/m$ (where E is the total energy per unit volume) can be expressed as

$$\varepsilon(\xi,\eta)=H_k[\sin^2(\xi/2)\cos^2(\eta)+\cos^2(\xi/2)\sin^2(\eta)] + \frac{H_1}{2}\cos(\xi)+\frac{H_2}{2}\cos^2(\xi) - 2H\cos(\xi/2)\cos(\psi-\eta), \tag{2}$$

where ξ is the angle between the two magnetic moments and η and ψ are the angles the net magnetization and applied magnetic field make with respect to the easy axis.[8] The magnetocrystalline, bilinear, and biquadratic coupling constants are given by

$$H_k\equiv\frac{2K_u}{m},\quad H_1\equiv\frac{2}{t}\frac{J_1}{m},\quad \text{and}\quad H_2\equiv\frac{2}{t}\frac{J_2}{m}, \tag{3}$$

where magnetocrystalline anisotropy K_u is assumed to be uniaxial, the bilinear coupling strength is given by J_1, and the biquadratic coupling strength by J_2.

The usual conditions for an energy minimum determine the equilibrium configuration and lead to coupled nonlinear differential equations that are easily solved in special cases, for example at high field, at zero field, or if $\eta=\pm\pi/2$. The saturation fields along the hard axis $H_{s,h}$ and the easy axis $H_{s,e}$ are given by

$$H_{s,h}=H_1+2H_2+H_k \quad \text{and} \quad H_{s,e}=H_1+2H_2-H_k. \tag{4}$$

The stable configurations at $H=0$, (ξ_0,η_0), are given by

$$(\xi_0,\eta_0)=\left[\arccos\left(\frac{H_k+H_1}{-2H_2}\right),\pm\frac{\pi}{2}\right] \quad \text{if} \quad 2H_2>H_k+H_1, \tag{5a}$$

$$(\xi_0,\eta_0)=(\pi,\pm\pi/2) \quad 0<2H_2\leqslant H_k+H_1, \tag{5b}$$

and

$$(\xi_0,\eta_0)=\left[\arccos\left(\frac{H_k-H_1}{2H_2}\right),0 \ \text{ or } \pi\right] \quad \text{if} \quad 2H_2>H_k-H_1, \tag{6a}$$

$$(\xi_0,\eta_0)=(0,0 \ \text{ or } \pi) \quad \text{if} \quad 0<2H_2\leqslant H_k-H_1. \tag{6b}$$

The configurations in Eq. (5) have a lower energy than those in Eq. (6) if the bilinear coupling is positive (i.e., it favors antiparallel alignment). Conversely, the configurations in Eq. (6) are favored for negative (ferromagnetic) bilinear coupling. In those configurations with $\eta=0$ or π, the net moment lies along the easy axis and the magnetocrystalline anisotropy acts to reduce ξ_0, whereas in the $\eta=\pm\pi/2$ configurations, the anisotropy acts to increase ξ_0. Consequently, the $\eta=0$ or π configurations can have a lower resistance than those with $\eta=\pm\pi/2$.

This analysis is based on a model of two magnetic layers while our data were taken on a multilayer with 20 ferromagnetic layers. To the extent that a 20 bilayer multilayer approximates an infinite multilayer,[9,16] Eq. (2) still describes the system but $H_1=(4/t)(J_1/m)$, and $H_2=(4/t)(J_2/m)$. For a finite multilayer, the outermost magnetic moments are coupled more weakly than the moments of the inner layers. Although this has a large effect on the spin-flop transition when the field is applied along the easy axis,[9] it is not important here and our data are well described by the model above.

The data in Fig. 2 for the $t_{\mathrm{Cu}}=10$ Å sample suggest that at zero field the magnetic moments of successive magnetic layers are alternately canted at $+\xi_0/2$ and $-\xi_0/2$ away from the easy axis of magnetization with $\eta=0$. The absence of a remnant magnetization for fields along the hard axis, seen in the Kerr data of Fig. 1, support this interpretation. The magnetization process pictured in Fig. 2 consistent with both the MR and Kerr data is this: at zero field the net magnetization must lie along the easy axis with $\xi_o<\pi/2$; when the field is increased along the hard axis the net magnetization moves to the hard axis as ξ opens to an angle $\xi>\xi_o$; finally, ξ closes to $\xi=0$ at the hard-axis saturation field, $H_{s,h}$. This is a reversible process.

Several conclusions can be drawn from the MR data. Considering Eqs. (5) and (6), it is clear that the observed MR minimum is a signature of biquadratic coupling and that because the MR is nonzero at zero field, $2H_2>H_k-H_1$. The MR minimum also indicates that the bilinear coupling is negative and favors the parallel alignment of adjacent magnetic layers.

One can estimate the values of H_2 and H_1 in the following way. Since the zero field angle is given by Eq. (6a), Eqs. (1), (4), and (6a) can be combined to give

$$H_2=\frac{H_{s,e}}{4\beta} \quad \text{and} \quad H_1=H_k+H_{s,e}\left[\frac{2\beta-1}{2\beta}\right], \tag{7}$$

where

$$\beta\equiv\left[\left(\frac{\Delta R(\xi=\xi_0)}{R_s}\right)\Big/\left(\frac{\Delta R(\xi_0=\pi)}{R_s}\right)\right],$$

the ratio of the MR at the minimum to the maximum MR the sample would attain if $\xi_0=\pi$. This is easily applied to the sample with $t_{\mathrm{Cu}}=10$ Å because the MR and magnetization data suggest that the sample with $t_{\mathrm{Cu}}=13$ Å is fully antiferromagnetically aligned at zero field. Neglecting the very small short circuiting effect of the extra Cu layers, this sets the MR scale for the sample with $t_{\mathrm{Cu}}=10$ Å so that $\beta=0.22$ and $\xi_0\approx56°$. In this sample $H_{s,h}$ and $H_{s,e}$ combine to give $H_2=1.08$ kOe and $H_1=-0.49$ kOe or $J_2\approx0.046$ ergs/cm^2 and $J_1\approx-0.021$ ergs/cm^2. For comparison, the sample with $t_{\mathrm{Cu}}=13$ Å has $J_1<0.047$ ergs/cm^2. Other researchers have modeled magnetoresistance curves in a similar fashion and extracted the coupling strengths by adjusting J_1 and J_2 to

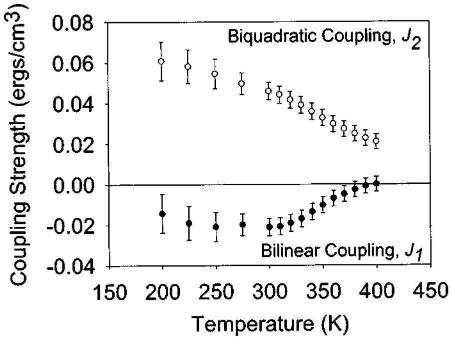

FIG. 3. The temperature dependence of the bilinear and biquadratic coupling constants for the NiFe/Cu multilayer with $t_{\mathrm{Cu}}=10$ Å.

obtain the best fit between the data and the predicted magnetization or MR curves.[17] The method described here differs from these techniques: we have identified the MR associated with the two zero-field states and solved uniquely for J_1 and J_2 without using adjustable parameters.

The solid line in Fig. 2 corresponds to the MR generated by numerically solving for the global energy minimum in Eq. (2) using the above values of H_1 and H_2. The data and simulation compare well, although the data are more rounded, probably because of a range of H_1 and H_2 values within the sample. The same process that leads to an MR minimum at zero field has been observed via magneto-optic imaging in a Fe/Cr system with fourfold magnetocrystalline anisotropy, for spacer-layer thicknesses very near the ferromagnetic bilinear coupling regime[3] and asymmetric states similar to those described above have been observed in Fe/Cr as well[18] and in NiFe/Ag.[19]

This experiment shows that the biquadratic coupling strength can be relatively strong in contrast with theories that predict the biquadratic coupling strength is smaller than the maximum in the bilinear coupling strength.[6,11,12] It seems difficult to reconcile these data with the fluctuation formalism as presented in Ref. 7 as well as the loose spin[13] and dipole mechanisms of biquadratic coupling.[14] In the Fe/Cr system, strong biquadratic coupling may arise from the proximity magnetism effect in the antiferromagnetic spacer layer.[20] This is not likely in a system with Cu spacer layers suggesting that another mechanism—one common to systems with magnetic and nonmagnetic spacer layers—may produce strong biquadratic coupling.

Using the technique described above we can measure the temperature dependence of the bilinear and biquadratic coupling strengths for the sample with $t_{\mathrm{Cu}}=10$ Å. As shown in Fig. 3 over the range of temperatures measured the bilinear coupling favors parallel alignment and is about half as strong as the biquadratic coupling. At high tempertures both J_1 and J_2 decrease with increasing temperature as expected; however, they have similar temperature dependences in contrast with measurements in a NiFe/Ag system.[21]

In the temperature range shown in Fig. 3 the sample with $t_{\mathrm{Cu}}=13$ Å attained the fully antiparallel orientation and, as mentioned above, served as the MR reference allowing us to determine J_1 and J_2 for the sample with $t_{\mathrm{Cu}}=10$ Å. However below 200 K the sample with $t_{\mathrm{Cu}}=13$ Å no longer attains the fully antiparallel configuration. In fact, at low temperatures the MR curve for the sample with $t_{\mathrm{Cu}}=13$ Å develops

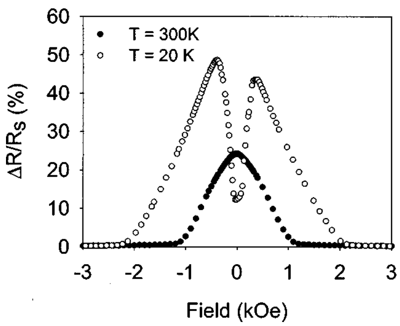

FIG. 4. Magnetoresistance curves for the NiFe/Cu sample with $t_{Cu} = 13$ Å when the field is applied along the hard axis. At room temperature the moments are coupled antiferromagnetically, as the shape of the room-temperature MR curve indicates. In contrast the MR minimum at low temperatures is indicative of strong biquadratic coupling and ferromagnetic bilinear coupling. The asymmetry in the MR curve at low temperatures results from the slight misalignment of the applied magnetic field relative to the sample's hard axis.

a low-field minimum as shown in Fig. 4. This indicates not only that the sample with $t_{Cu} = 13$ Å develops a strong biquadratic coupling term at low temperatures but also that the bilinear coupling changes sign from antiferromagnetic to ferromagnetic as the temperature is lowered below about 200 K. To our knowledge this is the first evidence for such a change of sign in the bilinear coupling term in transition-metal multilayers with nonmagnetic spacer layers.

Such a change of sign in the bilinear coupling term strongly suggests that the observed biquadratic does not result from fluctuation mechanism. In the fluctuation model indirect interlayer exchange coupling is responsible for both the ferromagnetically (F) and antiferromagnetically (AF) coupled regions. In the presence of the strong intralayer exchange, the F and AF regions contribute to the bilinear coupling in proportion to their area and also to biquadratic coupling. If the mechanisms for F and AF coupling are the same (namely indirect interlayer exchange coupling) then the sign of the bilinear coupling should be independent of temperature. Observation of a change of sign of the bilinear coupling term implies that the coupling mechanisms are different for the F and AF regions.

We propose that the ferromagnetically coupled regions arise from pinholes in the Cu spacer layer. The pinhole regions provide strong ferromagnetic coupling which when combined with regions of antiferromagnetic interlayer exchange coupling and strong intralayer coupling can lead to dominant biquadratic coupling.[20,22] The regions of ferromagnetic coupling also contribute to the measured bilinear coupling. The observed crossover from antiferromagnetic to ferromagnetic bilinear coupling as the temperature is reduced is a result of the increased stiffness of the ferromagnetic pinholes (which are believed to be more temperature dependent than the bulk material[23]).

Our work clearly demonstrates that the reentrant magnetoresistance results from biquadratic coupling and that, with few assumptions, the biquadratic and bilinear coupling strengths can be determined by resistance measurements alone. We have shown that systems with noble-metal spacer layers may have very strong biquadratic coupling, stronger than predicted by several existing theories. A crossover at low temperatures from antiferromagnetic to ferromagnetic bilinear coupling has been observed. This suggests that the ferromagnetic coupling, which in a frustration model is essential for biquadratic coupling, does not arise from interlayer exchange coupling. We propose that pinholes in the spacer layer are responsible for the ferromagnetic coupling.

The authors thank Kevin Roche and Arley Marley for their technical assistance. M.B.S. gratefully acknowledges support from Los Alamos National Laboratory. This work was preformed at IBM Almaden Research Laboratories and at the Materials Research Lab, University of Illinois and was funded in part by the DOE through Grant No. DEFG02-91ER45439.

[1] A. Fert and P. Bruno, in *Ultrathin Magnetic Structures II*, edited by B. Heinrich and J. A. C Bland (Springer, Berlin, 1994).
[2] S. S. P. Parkin, in *Ultrathin Magnetic Structures II*, edited by B. Heinrich and J. A. C Bland (Springer, Berlin, 1994).
[3] M. Rührig, R. Schäfer, A. Hubert, R. Mosler, J. A. Wolf, S. Demokritov, and P. Grünberg, Phys. Status Solidi A **125**, 635 (1991).
[4] D. T. Pierce, J. A. Stroscio, J. Unguris, and R. J. Celotta, Phys. Rev. B **49**, 14 564 (1994).
[5] B. Heinrich *et al.*, Phys. Rev. B **47**, 5077 (1993).
[6] J. Barnas, J. Magn. Magn. Mater. **126**, L21 (1993).
[7] J. C. Slonczewski, Phys. Rev. Lett. **67**, 3172 (1991).
[8] H. Fujiwara and M. R. Parker, J. Magn. Magn. Mater. **135**, L23 (1994); H. Fujiwara, IEEE Trans. Magn. **31**, 4112 (1995).
[9] N. S. Almeida and D. L. Mills, Phys. Rev. B **52**, 13 504 (1995).
[10] V. V. Ustinov *et al.*, Phys. Rev. B **54**, 15 958 (1996).
[11] D. M. Edwards, J. M. Ward, and J. Mathon, J. Magn. Magn. Mater. **126**, 380 (1993).
[12] R. P. Erickson, K. B. Hathaway, and J. R. Cullen, Phys. Rev. B **47**, 2626 (1993).
[13] J. C. Slonczewski, J. Appl. Phys. **73**, 5957 (1993).
[14] S. Demokritov, E. Tsymbal, P. Grünberg, W. Zinn, and I. K. Schuller, Phys. Rev. B **49**, 720 (1994).
[15] B. Briner and M. Landolt, Europhys. Lett. **28**, 65 (1994).
[16] B. Dieny, J. P. Gavigan, and J. P. Rebouillat, J. Phys.: Condens. Matter **2**, 159 (1990).
[17] U. Köbler, K. Wagner, R. Wiechers, A. Fuss, and W. Zinn, J. Magn. Magn. Mater. **103**, 236 (1992).
[18] A. Schreyer *et al.*, Phys. Rev. B **52**, 16 066 (1995).
[19] B. Dieny, S. Young, B. Rodmacq, J. Mouchot, M. H. Vaudaine, J. Magn. Magn. Mater. **162**, 38 (1996).
[20] J. C. Slonczewski, J. Magn. Magn. Mater. **150**, 13 (1995).
[21] B. Rodmacq, K. Dumesnil, P. Mangin, and M. Hennion, Phys. Rev. B **48**, 3556 (1993).
[22] J. F. Bobo, J. Fischer, and M. Piecuch, in *Magnetic Ultrathin Films, Multilayers and Surfaces/Interfaces and Characterization*, edited by B. T. Jonker *et al.*, MRS Symposia Proceedings No. 313 (Materials Research Society, Pittsburgh, 1993), p. 467.
[23] D. B. Fulghum and R. E. Camley, Phys. Rev. B **52**, 13 436 (1995).